

Minimalistic Attacks: How Little it Takes to Fool a Deep Reinforcement Learning Policy

Xinghua Qu¹, Zhu Sun¹, Pengfei Wei², Yew-Soon Ong¹, Abhishek Gupta³

¹Nanyang Technological University, Singapore; ²National University of Singapore;

³Singapore Institute of Manufacturing Technology;

{xinghua001,zhu.sun,asysong}@ntu.edu.sg, weipf@comp.nus.edu.sg, abhishek_gupta@simtech.a-star.edu.sg

Abstract

Recent studies have revealed that neural network based policies can be easily fooled by adversarial examples. However, while most prior works analyze the effects of perturbing every pixel of every frame assuming white-box policy access, in this paper we take a more minimalistic view towards adversary generation - with the goal of unveiling the limits of a model's vulnerability. In particular, we explore highly restrictive attacks considering *three key settings*: (1) *black-box policy access*: where the attacker only has access to the input (state) and output (action probability) of an RL policy; (2) *fractional-state adversary*: where only several pixels are perturbed, with the extreme case being a single-pixel adversary; and (3) *tactically-chanced attack*: where only significant frames are tactically chosen to be attacked. We formulate the adversarial attack by accommodating the three key settings, and explore their potency on six Atari games by examining four fully trained state-of-the-art policies. In Breakout, for example, we surprisingly find that: (i) all policies showcase significant performance degradation by merely modifying 0.01% of the input state, and (ii) the policy trained by DQN is totally deceived by perturbation to only 1% frames.

Introduction

Deep learning (Mnih et al. 2013) has been widely regarded as a promising technique in reinforcement learning (RL), where the goal of an RL agent is to maximize its expected accumulated reward by interacting with a given environment. Although deep neural network (DNN) policies have achieved super human performance on various challenging tasks (e.g., video games and board games), recent studies have shown that these policies are easily deceived under adversarial attacks (Huang et al. 2017; Lin et al. 2017; Yuan et al. 2019). These works are however found to make some common assumptions, viz., (1) white-box policy access: where the adversarial examples are analytically computed by back-propagating through known neural network weights, (2) full-state adversary: where the adversary changes almost all pixels in the state, and (3) fully-chanced attack: where the attacker strikes the policy at every frame.

Given that most prior works analyze the effects of perturbing every pixel of every frame assuming white-box policy access, in this paper we propose to take a more minimalistic view towards adversary generation - with the goal of

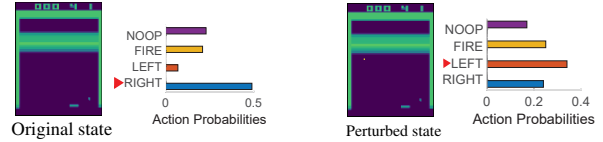


Figure 1: The minimalistic attack on Atari Breakout.

exploring the limits of a DNN model's vulnerability in RL. By defining minimalistic attacks, we intend to unveil how little it really takes to successfully fool state-of-the-art RL policies. To this end, we study adversarial attacks by considering three relatively restrictive settings, namely, *black-box policy access*, *fractional-state adversary*, and *tactically-chanced attack*. These concepts are detailed next.

Black-box Policy Access (BPA). Most previous studies focus on a white-box setting (Yuan et al. 2019), that allows full access to a policy network for back-propagation. However, most systems do not release their internal configurations (i.e. network structure and weights), only allowing the model to be queried; this makes the white-box assumption too optimistic from an attacker's perspective (Chen et al. 2017). In contrast, we use a BPA setting, where the attacker only has access to the input and output of a policy.

Fractional-State Adversary (FSA). In the FSA setting, the adversary only perturbs a small fraction of the input state. This, in the extreme situation, corresponds to the one-pixel attack shown in Fig. 1, where perturbing a single pixel of the input state is found to change the action prescription from 'RIGHT' to 'LEFT'. In contrast, most previous efforts (Yuan et al. 2019) are mainly based on a full-state adversary (i.e., the amount of modified pixels is fairly large).

Tactically-Chanced Attack (TCA). In previously studied RL adversarial attacks (Huang et al. 2017; Pattanaik et al. 2018; Pinto et al. 2017), the adversary strikes the policy on every frame of an episode; a setting that is termed as a fully-chanced attack. Contrarily, we investigate a relatively restrictive case where the attacker only strikes at a few selected frames - a setting we term as *tactically-chanced attack*, where a minimal number of frames is explored to strategically deceive the policy network.

The proposed restrictive settings are deemed to be significant for safety critical RL applications, such as in the medical treatment of sepsis patients in intensive care units (Raghu 2019; Raghu et al. 2017) and treatment strategies for

HIV (Parbhoo et al. 2017). In such domain, there may exist a temporal gap between the acquisition of the input and the action execution; thereby, providing a time window in which a tactical attack could take place. In the future, as we move towards integrating end-to-end vision-based systems for healthcare, the sensitivity of prescribed medical actions (such as drug prescription or other medical interventions) to minimalistic perturbations in medical images poses a severe threat to the utility of RL in such domains. Moreover, the restrictive nature of the attacks makes them practically imperceptible, greatly reducing the chance of identifying and rectifying them even in safety critical applications. With this in mind, the present paper explores the vulnerability of deep RL models to restrictive adversarial attacks, with particular emphasis on image-based tasks (i.e., Atari games).

We first formulate the RL adversarial attack task as a black-box optimization problem, where a novel objective function is designed to guarantee successful deceptions. Next, for investigating the FSA setting, the optimization variables are defined as the discrete 2-D coordinate location(s) and perturbation value(s) of the selectively attacked pixel(s). The optimization is then carried out by a simple genetic algorithm (GA) (Holland 1992; Deep et al. 2009). Finally, the Shannon entropy of the action distribution is specified as the attack significance, according to which only a minimalistic number of frames are tactically attacked. We demonstrate the efficacy of the three restrictive settings on four pre-trained state-of-the-art deep RL policies on six Atari games. Surprisingly, we find that on Breakout: (i) with **only** about 0.01% pixels attacked, the trained policies are completely deceived; and (ii) by merely attacking around 1% frames, the policy trained by DQN is totally fooled.

Related Work

Since (Szegedy et al. 2013), a number of adversarial attack methods have been investigated to fool deep neural networks (DNNs). Most existing approaches generate adversarial examples through pursuing human invisible perturbation on images, with the goal of deceiving trained classifiers. In other words, they mainly focus on the adversarial attacks for supervised learning tasks. Adversarial attacks in RL have been relatively less explored to date.

In RL, (Huang et al. 2017) were the first to demonstrate that neural network policies are vulnerable to adversarial attack by adding small modifications to the input state of Atari games. A full-state adversary (i.e. adversarial examples that change almost every pixel in the input state) has previously been generated by a white-box policy access based approach (Goodfellow, Shlens, and Szegedy 2014), where the adversarial examples are computed via back-propagation. (Lin et al. 2017) proposed the strategically-timed attack and the so-called enchanting attack, but the adversary generation is still based on white-box policy access assumption and full-state perturbation. In addition, (Kos and Song 2017) compare the influence of full-state perturbations with random noise, and utilize the value function to guide the adversary injection.

In summary, existing works are largely based on white-box policy access, together with assumptions of a full-state adversary and fully-chanced attack. There is little research

studying the potency of input perturbations that may be far less extensive, with the goal of investigating the vulnerability of deep RL models even in the face of minimalistic attacks (i.e., based on black-box policy access, fractional-state adversary, and tactically-chanced attack). It is contended that studying such restrictive scenario might give new insights on the geometrical characteristics and overall behavior of deep neural network in high dimensional spaces (Fawzi, Moosavi-Dezfooli, and Frossard 2017).

The Proposed Methodology

This section first provides preliminaries about existing adversarial attacks to DNN-based policies, and then presents the details of the three key settings for adversarial attack in RL, namely *black-box policy access* (BPA), *fractional-state adversary* (FSA), *tactically-chanced attack* (TCA).

Preliminaries

We first present the general formulation of adversarial attacks on deep RL. Let $r(\pi, s_t)$ represent a function that returns the reward given state s_t and DNN based policy π . The adversary generated at time-step t is represented by δ_t , the norm of which is assumed to be bounded by L . The aim of an RL adversarial attack is thus to find the optimal δ_t that minimizes the accumulated reward, given by,

$$\min_{\delta_t} \sum_{t=1}^T r(\pi, s_t + \delta_t) : \forall t \|\delta_t\| \leq L \quad (1)$$

where T is the length of an episode. Eq. (1) indicates that an action prediction a_t^p obtained from the perturbed state $s_t + \delta_t$ may differ from the originally unperturbed action a_t^o , thus jeopardizing the reward value $r(\cdot)$. This corresponds to the definition of untargeted attacks, which is stated as $a_t^o \neq a_t^p$.

To solve the mathematical program in Eq. (1), previous efforts (Huang et al. 2017; Lin et al. 2017) usually generate adversarial examples via white-box methods, e.g., FSGM (Goodfellow et al. 2017). These white-box methods are essentially gradient-based methods, as they generate adversarial examples by back-propagating through the RL policy to calculate the gradient of a cost function with respect to the input state, i.e. $\nabla_{s_t} J(\pi, \theta, \Delta a_t, s_t)$. Here, θ denotes the weights of the neural network; Δa_t indicates the change in action space; J is the cost function (e.g., cross-entropy loss).

A vital prerequisite of the white-box approach is the complete knowledge of the structure and the model parameters θ of the policy. In contrast, a more restrictive setting is marked by the black-box policy access (Chen et al. 2017), where the attacker sends the input state to the policy, which serves as an oracle to only provide the output action prediction.

Black-box Policy Access

We adopt the commonly used black-box definition (Chen et al. 2017; Su, Vargas, and Sakurai 2019) from supervised learning, where the attacker can only query the policy. In other words, the attacker is unable to analytically compute the gradient $\nabla_{s_t} \pi(\cdot | s_t, \delta_t)$, but only has the privilege to query a targeted policy in order to obtain useful information for crafting adversarial examples. However, such a setting has been rarely investigated in RL adversarial attacks.



(a) Full-state adversary (Goodfellow et al. 2017)

(b) Fractional-state adversary

Figure 2: Full-state adversary versus the FSA

We realize such a BPA setting by formulating the adversarial attack as a black-box optimization problem. To this end, we utilize a measure $\mathcal{D}(\cdot)$ to quantify the discrepancy between the original action distribution $\pi(\cdot|s_t)$ (produced by an RL policy under no input perturbation) and the corresponding perturbed $\pi(\cdot|s_t + \delta_t)$. The discrepancy measure is used as the optimization objective. Assuming a finite set of m available actions $a_t^1, a_t^2, \dots, a_t^m$, the probability distribution over actions is represented as $[p(a_t^1), p(a_t^2), \dots, p(a_t^m)]$, where $\sum_{j=1}^m p(a_t^j) = 1$. Hence, the black-box attack is formulated as perturbing the state s_t with δ_t , so as to maximize the discrepancy measure $\mathcal{D}(\cdot)$. The overall formulation is shown below:

$$\max_{\delta_t} \mathcal{D}(\pi(\cdot|s_t), \pi(\cdot|s_t + \delta_t)) : \forall t \|\delta_t\| \leq L \quad (2)$$

The above mathematical program changes the action distribution $\pi(\cdot|s_t + \delta_t)$ from the original (optimal) action distribution $\pi(\cdot|s_t)$. Based on Bellman’s principle of optimality (Sutton and Barto 2018), it can then be said that the perturbed action will lead to a sub-optimal reward as a consequence of the attack. Under this hypothesis, we propose to replace the reward minimization problem of Eq. (1) with a discrepancy maximization formulation proposed in Eq. (2).

The exact choice of discrepancy measure $\mathcal{D}(\cdot)$ is indeed expected to have a significant impact on the attack performance, as different measures shall capture different patterns of similarities. Many previous works apply the Euclidean norm (e.g., L_1, L_2, L_∞) between $\pi(\cdot|s_t + \delta_t)$ and $\pi(\cdot|s_t)$. However, such L_p norm cannot guarantee a successful untargeted attack, since maximizing L_p norm does not ensure that $\arg \max_j \pi(\cdot|s_t + \delta_t)_j \neq \arg \max_j \pi(\cdot|s_t)_j$, where $\pi(\cdot|s_t)_j = p(a_t^j)$.

To enable a more consistent discrepancy measure for untargeted attack, we design the following function $\tilde{\mathcal{D}}$ based on the query feedback of the policy.

$$\tilde{\mathcal{D}} = \max_{j \neq o} \pi(\cdot|s_t + \delta_t)_j - \pi(\cdot|s_t + \delta_t)_o \quad (3)$$

where: $o = \arg \max_j \pi(\cdot|s_t)_j$

This formulation is different from the Euclidean norm, guaranteeing a successful untargeted attack if $\tilde{\mathcal{D}}$ is positive. To support this claim, we refer to the theorem and proof below:

Theorem 1. *Suppose discrepancy measure $\tilde{\mathcal{D}}$ in Eq. (3) is positive with $\tilde{\mathcal{D}} > 0$; policy π is a deterministic, i.e., choosing action a_t^o such that $o = \arg \max_j \pi(\cdot|s_t)_j$. Then the adversarial example δ_t for policy π at state s_t , is guaranteed to make a successful untargeted attack, i.e.,*

$$\arg \max_j [\pi(s_t + \delta_t)]_j \neq \arg \max_j [\pi(s_t)]_j$$

Proof. We use the symbol o and p to represent the action index from state s_t and perturbed state $s_t + \delta_t$ respectively. As the policy π is deterministic, o and p are computed by:

$$o = \arg \max_j [\pi(\cdot|s_t)]_j$$

$$p = \arg \max_j [\pi(\cdot|s_t + \delta_t)]_j$$

The discrepancy measure $\tilde{\mathcal{D}}$ is positive, then we have

$$\tilde{\mathcal{D}} > 0 \Rightarrow \max_{j \neq o} \pi(\cdot|s_t + \delta_t)_j - \pi(\cdot|s_t + \delta_t)_o > 0$$

$$\Rightarrow \max_{j \neq o} \pi(\cdot|s_t + \delta_t)_j > \pi(\cdot|s_t + \delta_t)_o$$

$$\Rightarrow \max_j \pi(\cdot|s_t + \delta_t)_j = \max_{j \neq o} \pi(\cdot|s_t + \delta_t)_j$$

Therefore, the perturbed action index p is given by:

$$p = \arg \max_j \pi(\cdot|s_t + \delta_t)_j = \arg \max_{j \neq o} \pi(\cdot|s_t + \delta_t)_j \neq o$$

$$\Rightarrow \arg \max_j [\pi(\cdot|s_t + \delta_t)]_j \neq \arg \max_j [\pi(\cdot|s_t)]_j \quad \blacksquare$$

With the discrepancy measure $\tilde{\mathcal{D}}$, the mathematical program for generating adversarial attacks is given by,

$$\max_{\delta_t} \max_{j \neq o} \pi(\cdot|s_t + \delta_t)_j - \pi(\cdot|s_t + \delta_t)_o \quad (4)$$

where: $\forall t \|\delta_t\| \leq L, o = \arg \max_j \pi(\cdot|s_t)_j$

When resolving the mathematical program in Eq. (2), δ_t is determined by its parameterisation. In this paper, the adversary δ_t is limited to perturbing only a small fraction of the input state (i.e. fractional-state adversary), described next.

Fractional-State Adversary

To explore adversarial attacks limited to a few pixels in RL, we investigate the fractional-state adversary (FSA) setting. In comparison with the full-state adversary depicted in Figure 2(a), FSA only perturbs a fraction of the state; shown in Figure 2(b). The extreme scenario for FSA is merely a single-pixel attack, which is deemed to be more physically realizable for the attacker than a full-state one. For instance, pasting a sticker or a simple fading of color in the “STOP” sign could easily lead to a FSA in Figure 2(b).

We parameterize the adversary δ_t by its corresponding pixel coordinates (i.e. $\mathbf{x}_t, \mathbf{y}_t$) and perturbation value \mathbf{p}_t :

$$\delta_t = \mathcal{P}(\mathbf{x}_t, \mathbf{y}_t, \mathbf{p}_t)$$

$$= \mathcal{P}(x_t^1, y_t^1, p_t^1, \dots, x_t^n, y_t^n, p_t^n) \quad (5)$$

where n is the number of pixels that are attacked, x_t^i, y_t^i are coordinate values of the its selected pixel, and p_t^i is the adversarial perturbation value of that pixel. With Eq. (5), the final black-box optimization problem is formulated as:

$$\max_{\mathbf{x}_t, \mathbf{y}_t, \mathbf{p}_t} \max_{j \neq o} [\pi(\cdot|s_t + \mathcal{P}(\mathbf{x}_t, \mathbf{y}_t, \mathbf{p}_t))]_j - [\pi(\cdot|s_t + \mathcal{P}(\mathbf{x}_t, \mathbf{y}_t, \mathbf{p}_t))]_o$$

where: $\forall t o = \arg \max_j [\pi(\cdot|s_t)]_j$

$$\forall t 0 \leq x_t^i \leq \mathcal{I}_x, x_t^i \in \mathbb{N}, i = [1, 2, \dots, n];$$

$$\forall t 0 \leq y_t^i \leq \mathcal{I}_y, y_t^i \in \mathbb{N}, i = [1, 2, \dots, n];$$

$$\forall t 0 \leq p_t^i \leq \mathcal{I}_p, p_t^i \in \mathbb{N}, i = [1, 2, \dots, n];$$

(6)

Algorithm 1: Attack by Genetic Algorithm

Input: s_t – state at time-step t ; n – number of pixels for attack; λ – population size; β – rate of elitism; γ – rate of mutation; f_m – maximum number of function evaluations; ζ^* – TCA boundary value

```

1 Load the policy  $\pi$  well-trained by a particular RL algorithm;
2 Obtain the RL input state  $s$  in a particular Atari game;
3 Calculate the attack significance  $\zeta_t$  by Eq. (7);
4 if  $\zeta \geq \zeta^*$  then
    // No adversarial attack
     $\delta_t = \text{none}$ ;
5 else
    // Explore the  $n$  pixel attack
    Initialize the population  $pop$  with randomly generating
     $\lambda$  individuals;
6 repeat
    Evaluate  $f_i, i = 1, \dots, \lambda$  using Eq. (6);
    Save the top- $\lambda\beta$  individuals in  $pop'$ ;
7   for  $j=1: \frac{\lambda(1-\beta)}{2}$  do
    Crossover: generate  $\delta_c^j$  with one-point
    crossover (Holland 1992);
    Mutation:  $\delta_m^j = \delta^j + \gamma \cdot \epsilon_j, \epsilon_j \in \mathcal{N}(0, 1)$ ;
8   Append  $\delta_c$  and  $\delta_m$  to  $pop'$ ;
9    $pop = pop'$ 
10 until the maximum objective evaluations  $f_m$  reached;
11 Return the optimal FSA  $\delta^* = [\mathbf{x}^*, \mathbf{y}^*, \mathbf{p}^*]$ ;

```

where $\mathcal{I}_x, \mathcal{I}_y$ are the integral upper bounds of \mathbf{x}_t and \mathbf{y}_t respectively, \mathcal{I}_p is the perturbation value bound of \mathbf{p}_t , and n is the FSA size that controls the number of pixels to be attacked given any input state s_t . In the extreme case $n = 1$, there is only *one pixel* attacked in a frame. To the best of our knowledge, such one-pixel attack has never been explored in the existing literature on RL adversarial attacks.

To obtain the optimal $\mathbf{x}_t, \mathbf{y}_t, \mathbf{p}_t$, we adopt a simple genetic algorithm (GA) (Holland 1992; Bertsekas 1997; Deep et al. 2009), a derivative-free method to solve black-box optimization problems of the type in Eq. (6). The pseudo code of GA is illustrated in Algorithm 1 (lines 7-17). A population of λ individuals δ_t is evolved, where each δ_t is a particular adversarial example that is evaluated by the objective function in Eq. (6). The top- $\lambda\beta$ individuals with respect to the objective value, are selected as elites to survive in the new generation (line 10). Based on standard crossover (line 12) and mutation (line 13) operations, another population pop' is reproduced to replace the old pop . This process repeats until the maximum objective evaluation number f_m is reached.

Tactically-Chanced Attack

To explore the adversarial attacks on a limited number of frames, we design the tactically-chanced attack (TCA) where the attacker strategically strikes *only* significant frames. In contrast, most existing approaches (Huang et al. 2017) apply adversarial examples on every frame, which is referred to as the fully-chanced attack. Our proposed TCA is more minimalistic from three perspectives: (1) due to the communication budget restriction, the attacker may not be able to strike the policy in a fully-chanced fashion; (2) a tactically-chanced attack is less likely to be detected by the

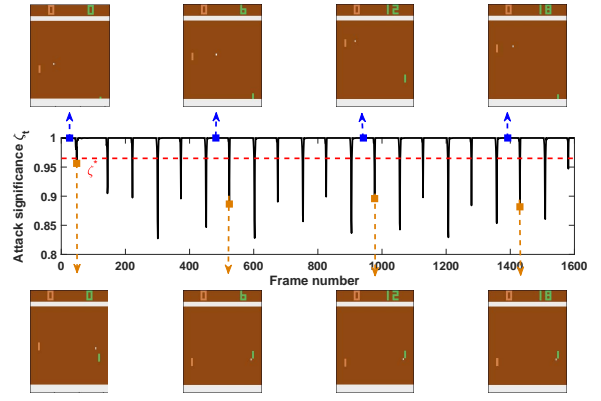


Figure 3: The attack significance ζ_t on Pong.

defender; and (3) striking on the significant frames only improves the attack efficiency, as many frames contribute trivially to the accumulated reward.

To this end, we define the normalized Shannon entropy of the action distribution $\pi(\cdot|s_t) = [p(a_t^1), p(a_t^2), \dots, p(a_t^m)]$ to measure the attack significance. Such attack significance (ζ_t) of each frame is given by,

$$\zeta_t = - \sum_{i=0}^m \frac{p(a_t^i) \cdot \log p(a_t^i)}{\log m} \quad (7)$$

where $p(a_i)$ is the probability of action a_i ; m is the dimension of the action space. As probability $p(a_i)$ falls in $[0, 1]$, ζ_t is constrained in $(0, 1]$. In such a formulation, the frame with relatively low ζ_t indicates that the policy has a high confidence in its prescribed action. Hence, attacking such frames is expected to effectively disrupt the policy.

We demonstrate the attack significance on Pong in Figure 3; similar trends can be observed on the other games as well. In the figure, the frames with smaller ζ_t , marked by brown rectangles, depict that the ball is close to the paddle. On the other hand, the blue rectangle marked ones with large ζ_t (around 1) indicate that the ball is distant from the paddle. Attacking the brown marked frames are intuitively more significant for the policy, as they are likely to lead to a more considerable reward loss. In contrast, an attack may be relatively inconsequential for the blue marked frames. As the ball is distant from the paddle, attacking such frames will have little impact on the reward.

Therefore, we formulate the TCA by defining a TCA threshold (ζ^*) as shown by the red line in Figure (3); this controls the proportion of attacked frames as only those frames with a significance value below ζ^* are perturbed. In the experimental section we analyze the effect of different values of the threshold ζ^* , which also helps us to explore how little it may actually take to deceive a policy (from the perspective of the number of frames attacked). The adversary δ_t under TCA setting is given by:

$$\delta_t = \begin{cases} \mathcal{P}(\mathbf{x}_t^*, \mathbf{y}_t^*, \mathbf{p}_t^*), & \text{if } \zeta_t < \zeta^* \\ \text{none}, & \text{if } \zeta_t \geq \zeta^* \end{cases} \quad (8)$$

Eq. (8) suggests that if the attack significance (ζ_t) is smaller than ζ^* , an adversary shall be generated by solving the optimization task in Eq. (6). Otherwise, the attacker will tactically hide without wasting sources on trivial frames.

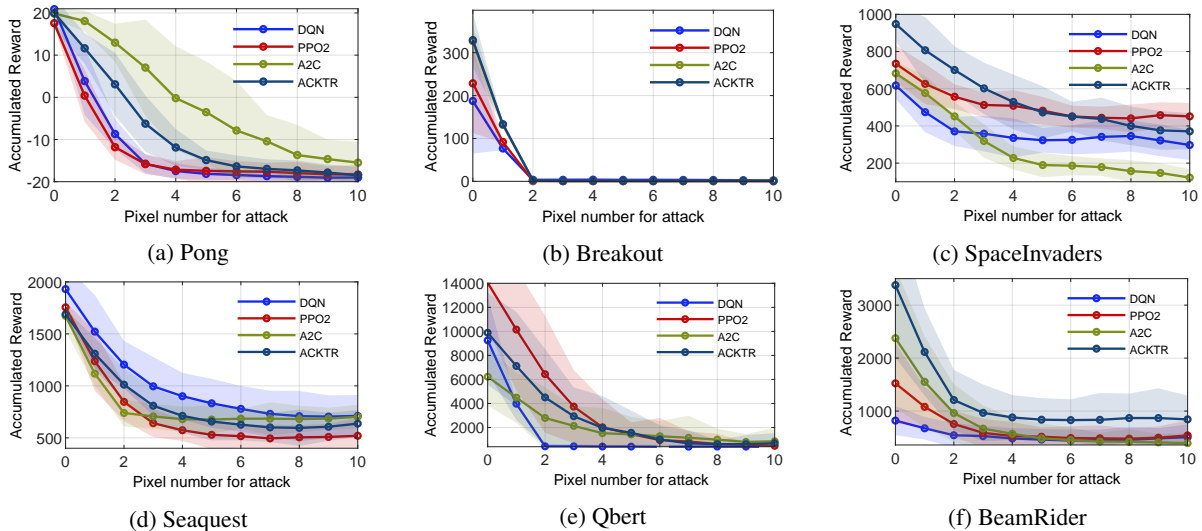


Figure 4: The results of adversarial attack with different FSA size n (i.e. pixel number), where the line and shaded area illustrate the mean and stand deviation of 30 independent runs respectively.

Summary. By considering the three settings (i.e., BPA, FSA and TCA), we carry out an exploration of restrictive scenarios for RL adversarial attacks, only focusing on a minimal number of pixels and frames under black-box policy access.

Experiments

We evaluate the three restrictive settings on six Atari games in OpenAI Gym (Brockman et al. 2016) with various difficulty levels, including Pong, Breakout, SpaceInvaders, Seaquest, Qbert, and BeamRider. These games are shown in Figure S1 in Appendix A. For each game, the policies are trained by four start-of-the-art RL algorithms, including DQN (Mnih et al. 2013), PPO2 (Schulman et al. 2017), A2C (Mnih et al. 2016), ACKTR (Wu et al. 2017). These RL training algorithms are listed in Appendix B with details¹.

Experiment Setup

We utilize the fully-trained policies from the RL baseline zoo (RAFFIN 2018). Each policy follows the same pre-processing steps and neural network architecture in (Mnih et al. 2013). The input state s_t of the neural network is the concatenation of the last four screen images, where each image is resized to 84×84 . The pixel value of the grey scale image is in the range of $[0, 255]$ stepped by 1. The output of the policy is a distribution over candidate actions for PPO2, A2C, ACKTR, and an estimation of Q values for DQN.

To calculate the attack significance for DQN, the softmax operation is applied to normalize the output. Moreover, given the image size and pixel value, the constraints in Eq. (6) are set as $\mathcal{I}_x = 84$, $\mathcal{I}_y = 84$, $\mathcal{I}_p = 255$. In GA, the population size $\lambda = 10$, and maximum objective evaluation $f_m = 400$. However, as our objective has a guarantee for successful untargeted adversarial attack, the optimization process will terminate when positive objective is found. To investigate the impacts of FSA size n , we apply a grid

search in $[1, 10]$ scaled by 1. We also apply a grid search for tactically-chanced attack (TCA) threshold ζ^* in the range of $[0, 1]$. This corresponds to the different proportion of attacked frames as depicted by the x-axis in Figure 5.

Results for Fractional-State Adversary

We investigate the effectiveness of the fractional-state adversary (FSA) via varying the value of FSA size n in the range of $[1, 10]$ scaled by 1, where $n = 1$ corresponds to the extreme case that only one pixel is perturbed. For a fair comparison w.r.t. different algorithms and games, we set the TCA threshold ζ^* as the mean of all frames' ζ that are obtained from the unattacked policy testing. Figure 4 illustrates the performance (i.e. accumulated reward) drop on the policies trained by the four RL algorithms on the six Atari games. Several interesting observations can be noted.

(1) Overall, the FSA size n is positively related to the performance drop. That is to say, the FSA with larger n is easier to deceive the policy to lose reward, *vice versa*. (2) On most of the games, the policies are almost completely fooled with $n \leq 4$. This indicates a small FSA size is able to achieve a successful adversarial attack, indicating the efficiency of FSA. (3) There is a relatively huge performance drop for DQN based policy in comparison with policies trained by other RL algorithms, especially on Breakout and Qbert. It suggests that DQN based policy is much easier to be attacked; whereas, the ACKTR based policy is more robust under the attack with FSA setting. (4) The results also imply that the high performance of unattacked policy cannot guarantee a strong robustness to resist attack. For instance, in SpaceInvaders, the original performance of A2C is higher than DQN, but the performance of A2C drops faster than that of DQN as shown in Figure 4(c). (5) Most importantly, we *surprisingly* find that: on Breakout, with single pixel attacked, the policy trained by all the four RL algorithms are completely deceived with the accumulated reward close to 0; On Qbert and BeamRider, the policy trained by DQN is also completely deceived with only single pixel attacked. Such

¹Our code is at <https://github.com/RLMA2019/RLMA>

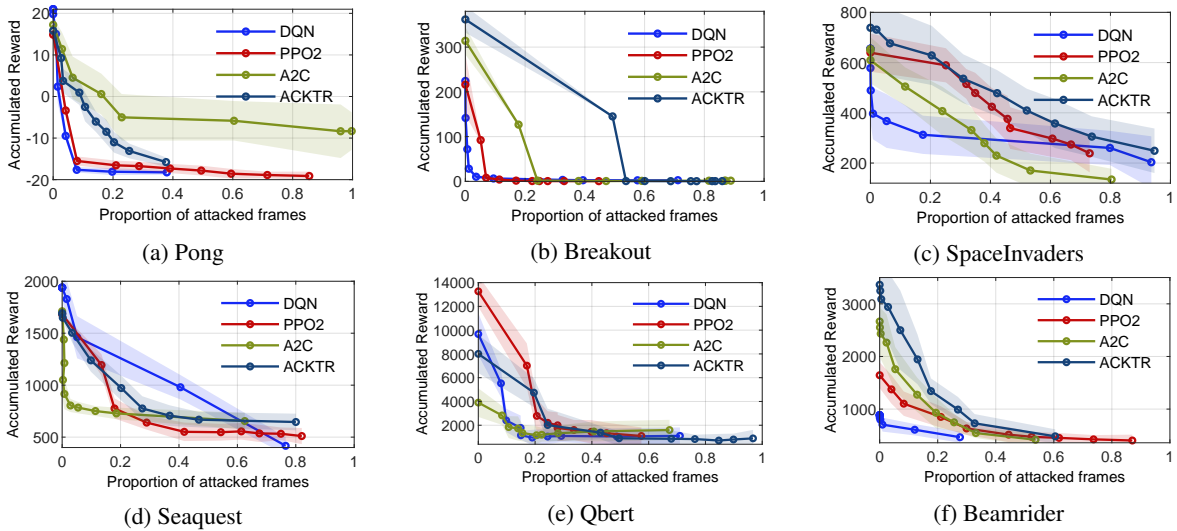


Figure 5: The results of adversarial attack with different TCA boundary ζ^* , where the line and shaded area illustrate the mean and stand deviation of 30 independent runs respectively.

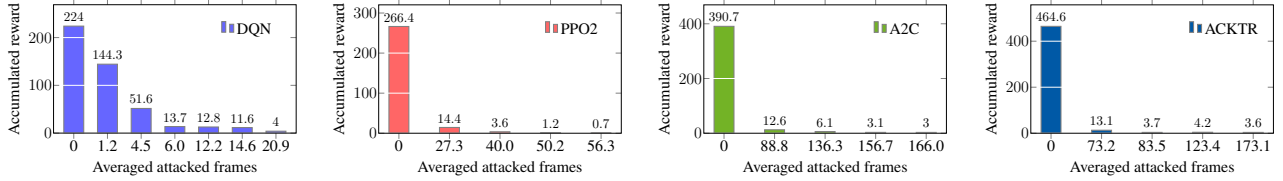


Figure 6: The impact of attacked frames for accumulated reward on Breakout

single pixel attack corresponds to an approximate perturbation proportion 0.01% (i.e., $1/(84 \times 84)$) among total pixels.

Results for Tactically-Chanced Attack

We study the tactically-chanced attack (TCA) via altering the TCA threshold ζ^* . Different ζ^* corresponds to different proportion of attacked frames among the total frames. To explore different proportions of attacked frames, we set the ζ^* in the range of $(0, 1]$, where $\zeta^* = 0$ and $\zeta^* = 1$ correspond to 0% and 100% proportion of attacked frames respectively. Additionally, according to the results for FSA size analysis shown in Figure 4, most of the policies are clearly fooled with no more than 4 pixels attacked. Hence, for a fair comparison, we set the FSA size $n = 4$. The results are displayed in Figure 5, where we observe that in general the performance (i.e., accumulated reward) decreases when higher proportion of frames are attacked. This suggests that the policies are easier to be fooled with more frames attacked. In particular, we achieve several fascinating findings.

(1) In Figure 5(a) on Pong, only with around 10% of frames attacked, the models trained by DQN and PPO2 are deeply fooled with the accumulated reward around -20 . It also suggests that the model trained by A2C and ACKTR are more robust than those trained by DQN and PPO2. (2) In Figure 5(b) on Breakout, the model trained by DQN is deeply deceived with only perturbing less than 5% of frames on average. Meanwhile, all the policies trained by the four RL algorithms witness a significant performance drop,

when the proportions of attacked frames increase. (3) In Figure 5(f) on Beamrider, with the proportion reaching around 20%, all the policies obtain less than 2000 points. Especially for the policies trained by DQN and PPO2, the accumulated reward drops to 2000 from 14000 or so.

To explore a more restrictive setting, we further examine the single-pixel ($n = 1$) attack on limited frames. Due to the space limitation, we only illustrate the results on Breakout as shown in Figure 6. From this figure, we surprisingly find that with only attacking on six frames averagely, the policy trained by DQN is totally fooled with reward decreasing from 224 to 13.7. Here, six frames correspond to an attack ratio of $6/535 \approx 1\%$, where 535 is the averaged number of total frames. Similar surprising findings are also observed on policies trained by PPO2, A2C and ACKTR. For instance, the policy trained by PPO2 shows a significant reward decline with only 27 frames attacked.

Further, we analyze the exact number of attacked frames with different TCA threshold values that represent different proportion of attacked frames. As shown in Figure 7, the number of attacked frames increases when the proportion value is higher. In Figure 7 (b), on Breakout, when the proportion value is smaller than 20%, less than 50 frames are attacked. The same finding is also observed on Beamrider, where less than 100 frames are attacked when the proportion value is smaller than 20%. On Pong, to achieve a same reward degradation, the policy trained by A2C requires more frames attacked than that of the other three RL policies.

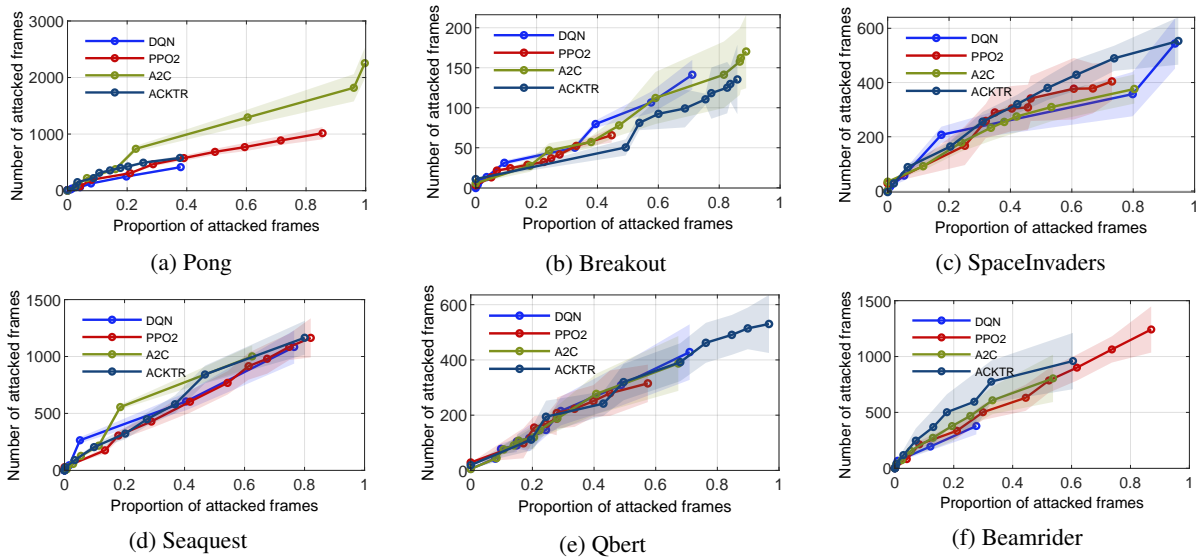


Figure 7: The relationship between attacked frames and total frames, where the line and shaded area illustrate the mean and stand deviation of 30 independent runs respectively.

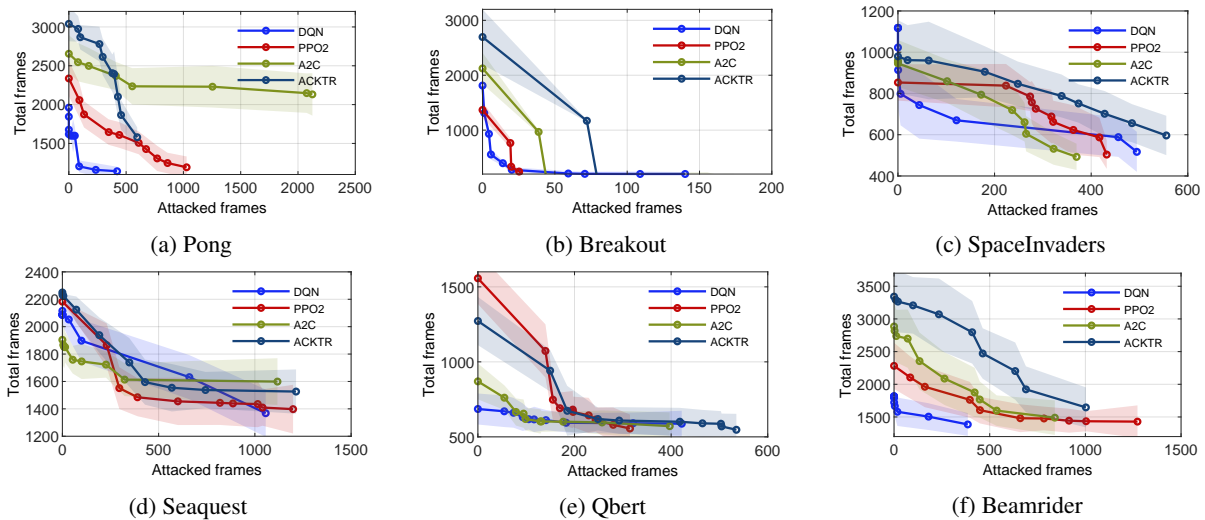


Figure 8: The relationship between attacked frames and total frame, where the line and shaded area illustrate the mean and stand deviation of 30 independent runs respectively.

Last but not the least, we analyze the relationship between attacked frames and total frames in Figure 8. We find a same trend on the six games, where the number of total frames decreases when more frames are attacked. In particular, such relationship is significantly observed on Breakout, where less than 50 frames attacked considerably reduce the number of total frames to a small value from 2000 or so. This is probably produced by the fact that, the attacked frame may cause (i) the termination of the game, or (ii) a lost of life (evaluation episodes still lasted for the entire game). Both outcomes greatly decrease the length of the episode, resulting a smaller number of total frames. For instance, if the paddle in Breakout is deceived to miss the ball, the agent would lose 1/5 life. In summary, the results and analyses suggest that by moderately setting the FSA size and TCA threshold, the attacker could efficiently strikes the policy.

Conclusion

This paper explores the *restricted scenario* for adversarial attack in reinforcement learning (RL) with **three settings**: (1) black-box policy access that the attacker only has access to the input (state) and output (action probability) of an RL policy; (2) fractional-state adversary that only a small number of pixels are perturbed where the extreme case is the one-pixel attack; and (3) tactically-chanced attack that only significant frames are smartly chosen to be attacked. We verify these settings on policies that are trained by four state-of-the-art RL policies on six Atari games. We surprisingly find that: (1) the models trained by all RL algorithms on Breakout are significantly fooled by merely modifying 0.014% of the input state; and (2) the policy trained by DQN is totally deceived via single-pixel attack to only six frames (i.e. 1%).

References

- [Bertsekas 1997] Bertsekas, D. P. 1997. Nonlinear programming. *Journal of the Operational Research Society* 48(3):334–334.
- [Brockman et al. 2016] Brockman, G.; Cheung, V.; Pettersson, L.; Schneider, J.; Schulman, J.; Tang, J.; and Zaremba, W. 2016. Openai gym. *arXiv preprint arXiv:1606.01540*.
- [Chen et al. 2017] Chen, P.-Y.; Zhang, H.; Sharma, Y.; Yi, J.; and Hsieh, C.-J. 2017. Zoo: Zeroth order optimization based black-box attacks to deep neural networks without training substitute models. In *Proceedings of the 10th ACM Workshop on Artificial Intelligence and Security*, 15–26. ACM.
- [Deep et al. 2009] Deep, K.; Singh, K. P.; Kansal, M. L.; and Mohan, C. 2009. A real coded genetic algorithm for solving integer and mixed integer optimization problems. *Applied Mathematics and Computation* 212(2):505–518.
- [Fawzi, Moosavi-Dezfooli, and Frossard 2017] Fawzi, A.; Moosavi-Dezfooli, S.-M.; and Frossard, P. 2017. The robustness of deep networks: A geometrical perspective. *IEEE Signal Processing Magazine* 34(6):50–62.
- [Goodfellow et al. 2017] Goodfellow, I.; Papernot, N.; Huang, S.; Duan, Y.; Abbeel, P.; and Clark, J. 2017. Attacking machine learning with adversarial examples. *OpenAI*. <https://blog.openai.com/adversarial-example-research>.
- [Goodfellow, Shlens, and Szegedy 2014] Goodfellow, I. J.; Shlens, J.; and Szegedy, C. 2014. Explaining and harnessing adversarial examples. *arXiv preprint arXiv:1412.6572*.
- [Holland 1992] Holland, J. H. 1992. Genetic algorithms. *Scientific american* 267(1):66–73.
- [Huang et al. 2017] Huang, S.; Papernot, N.; Goodfellow, I.; Duan, Y.; and Abbeel, P. 2017. Adversarial attacks on neural network policies. *arXiv preprint arXiv:1702.02284*.
- [Kos and Song 2017] Kos, J., and Song, D. 2017. Delving into adversarial attacks on deep policies. *arXiv preprint arXiv:1705.06452*.
- [Lin et al. 2017] Lin, Y.-C.; Hong, Z.-W.; Liao, Y.-H.; Shih, M.-L.; Liu, M.-Y.; and Sun, M. 2017. Tactics of adversarial attack on deep reinforcement learning agents. *arXiv preprint arXiv:1703.06748*.
- [Mnih et al. 2013] Mnih, V.; Kavukcuoglu, K.; Silver, D.; Graves, A.; Antonoglou, I.; Wierstra, D.; and Riedmiller, M. 2013. Playing atari with deep reinforcement learning. *arXiv preprint arXiv:1312.5602*.
- [Mnih et al. 2016] Mnih, V.; Badia, A. P.; Mirza, M.; Graves, A.; Lillicrap, T.; Harley, T.; Silver, D.; and Kavukcuoglu, K. 2016. Asynchronous methods for deep reinforcement learning. In *International conference on machine learning*, 1928–1937.
- [Parbhoo et al. 2017] Parbhoo, S.; Bogojeska, J.; Zazzi, M.; Roth, V.; and Doshi-Velez, F. 2017. Combining kernel and model based learning for hiv therapy selection. *AMIA Summits on Translational Science Proceedings* 2017:239.
- [Pattanaik et al. 2018] Pattanaik, A.; Tang, Z.; Liu, S.; Bommannan, G.; and Chowdhary, G. 2018. Robust deep reinforcement learning with adversarial attacks. In *Proceedings of the 17th International Conference on Autonomous Agents and MultiAgent Systems*, 2040–2042. International Foundation for Autonomous Agents and Multiagent Systems.
- [Pinto et al. 2017] Pinto, L.; Davidson, J.; Sukthankar, R.; and Gupta, A. 2017. Robust adversarial reinforcement learning. In *Proceedings of the 34th International Conference on Machine Learning-Volume 70*, 2817–2826. JMLR. org.
- [RAFFIN 2018] RAFFIN, A. 2018. Reinforcement learning baseline zoo. <https://github.com/araffin/rl-baselines-zoo>.
- [Raghu et al. 2017] Raghu, A.; Komorowski, M.; Celi, L. A.; Szolovits, P.; and Ghassemi, M. 2017. Continuous state-space models for optimal sepsis treatment—a deep reinforcement learning approach. *arXiv preprint arXiv:1705.08422*.
- [Raghu 2019] Raghu, A. 2019. Reinforcement learning for sepsis treatment: Baselines and analysis. *Reinforcement Learning for Real Life*.
- [Schulman et al. 2017] Schulman, J.; Wolski, F.; Dhariwal, P.; Radford, A.; and Klimov, O. 2017. Proximal policy optimization algorithms. *arXiv preprint arXiv:1707.06347*.
- [Su, Vargas, and Sakurai 2019] Su, J.; Vargas, D. V.; and Sakurai, K. 2019. One pixel attack for fooling deep neural networks. *IEEE Transactions on Evolutionary Computation*.
- [Sutton and Barto 2018] Sutton, R. S., and Barto, A. G. 2018. *Reinforcement learning: An introduction*. MIT press.
- [Szegedy et al. 2013] Szegedy, C.; Zaremba, W.; Sutskever, I.; Bruna, J.; Erhan, D.; Goodfellow, I.; and Fergus, R. 2013. Intriguing properties of neural networks. *arXiv preprint arXiv:1312.6199*.
- [Wu et al. 2017] Wu, Y.; Mansimov, E.; Grosse, R. B.; Liao, S.; and Ba, J. 2017. Scalable trust-region method for deep reinforcement learning using kronecker-factored approximation. In *Advances in neural information processing systems*, 5279–5288.
- [Yuan et al. 2019] Yuan, X.; He, P.; Zhu, Q.; and Li, X. 2019. Adversarial examples: Attacks and defenses for deep learning. *IEEE transactions on neural networks and learning systems*.

Appendix A: The Atari games evaluated

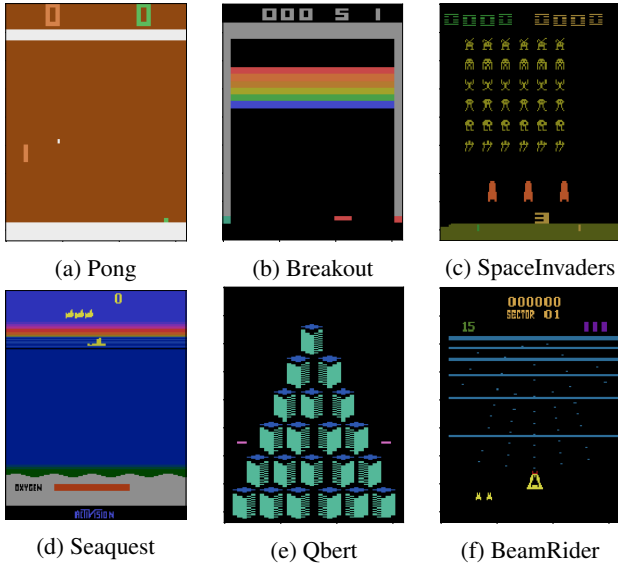


Figure S1: The six representative Atari games (i.e., Pong, Breakout, SpaceInvaders, Seaquest, Qbert, BeamRider) applied in the experiments

Appendix B: The RL algorithms evaluated

Reinforcement learning algorithms train a policy π to maximize the expected cumulative reward received. In our paper, such policy π is a deterministic model that maps the state s to a predicted action a . Over the past decades, many different RL algorithms have been proposed. We select several representative ones, i.e., Deep Q-Networks (DQN) (Mnih et al. 2013), PPO (Schulman et al. 2017), A2C (Mnih et al. 2016), ACKTR (Wu et al. 2017).

- **Deep Q-Networks (DQN) (Mnih et al. 2013):** Instead of predicting the probability of each action, DQN computes the Q value for each available action. Such Q value $Q^*(s, a)$ represents the approximated expected cumulative discounted reward that obtained since the current frame. Based on such approximation, the DQN is trained via minimizing the temporal difference loss (i.e., squared Bellman error). In this paper, the corresponding policy for DQN is achieved by selecting the action with maximum Q value. In addition, to make the prediction of DQN consistent with other policies, a soft-max layer is added after the output of DQN.
- **Proximal Policy Optimization (PPO)(Schulman et al. 2017):** PPO is an off-policy method using policy gradient, and it strikes a balance between ease of implementation, sample complexity, and ease of tuning. PPO is proposed based on trust region policy optimization (TRPO), but PPO much simpler to implement, more general, and have better sample complexity (empirically). PPO tries to compute an update at each step with minimizing the cost function while restricting the updating step to be relatively small. To this end, in the loss function, PPO involves in a penalty term that indicates the Kullback-

Leibler divergence between old policy action prediction and the new one.

- **Advantage Actor-Critic (A2C) (Sutton and Barto 2018):** A2C is an actor-critic method that learns both a policy and a state value function (i.e., also called critic). Such design is to reduce variance and accelerate learning with updating a state from subsequent estimation. The advantage A means a function value that is formulated by $A = Q(s_t, a_t) - V(s_t)$, where $Q(s_t, a_t)$ is the state-action value and $V(s_t)$ is the state value.
- **Actor Critic using Kronecker-Factored Trust Region (ACKTR) (Wu et al. 2017):** ACKTR is an extension of the natural policy gradient, and it optimizes both the actor and the critic using Kronecker-factored approximate curvature (K-FAC) with trust region. It is the first scalable trust region natural gradient method for actor-critic methods. It suggests that Kronecker-factored natural gradient approximations in reinforcement learning is a promising framework.